Low-temperature electrochemical ammonia synthesis: recent progress and comparison to Haber-Bosch in terms of energy efficiency

Fateme Rezaie[1], Nihat Ege Sahin[1], Søren Læsaa[1], Jacopo Catalano,[1] Emil Drazevic[1,*]

Fateme Rezaie (frezaie@bce.au.dk), Nihat Ege Sahin (nsahin@bce.au.dk), Søren Læsaa (laesaa@bce.au.dk), Jacopo Catalano (jcatalano@au.dk), Emil Drazevic (edrazevic@bce.au.dk)
[1]Aarhus University, Department of Biological and Chemical Engineering, Aabogade 40, 8200 Aarhus N, Denmark

Graphical Abstract

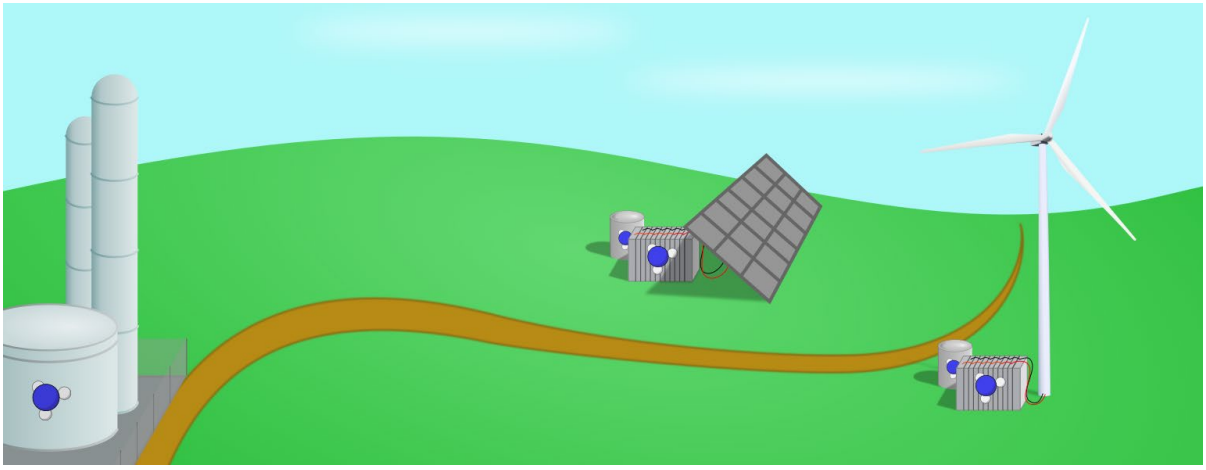

Abstract

The electrochemical synthesis of ammonia, in the literature often referred to as Electrochemical Nitrogen Reduction Reaction (ENRR), has gained attention as a milder alternative to the Haber-Bosch process, which requires high temperature and pressure. Recently, several breakthrough scientific papers were published showing a way to achieve nearly 100% selectivity of the ENRR over hydrogen reduction at very high production rates, which had been identified earlier as a main challenge. These results motivated the present study to benchmark the energy efficiencies of the most reliable ENRR studies against the Haber-Bosch process. ENRR studies historically suffered from reliability issues due to low ammonia production rates, which were often within the range of ambient ammonia contamination, potentially leading to false positive measurements. Consequently, rigorous experimental protocols have been published in the last four years. Here we first reviewed the protocols and established a methodology and a reliability indicator to assess the reliability of the results. Then we used the indicator to evaluate the studies reported in the literature from January 2019 to Aug 2022. Finally, we discussed and calculated the energy efficiency of ENRR for works that were assessed as *reliable and probably reliable* with the indicator. We identified and discussed several promising systems and strategies enabling higher energy efficiency. The energy efficiency had a maximum of 41%, which is within the efficiency range of current Haber-Bosch plants. However, ENRR energy efficiencies must improve to get closer to the 56% some of the state-of-the art Haber-Bosch plants achieve.

Introduction

Green ammonia can be produced using a Haber-Bosch loop combined with a renewable-energy-powered electrolyser as a source of green hydrogen. Hydrogen and dinitrogen separated from air are reacted to form green liquid anhydrous ammonia. Here "green" means ammonia is produced in a sustainable way. This process is energy efficient and proceeds at high pressures (150-300 bar) and high temperatures (350-520 °C).[1] The Haber-Bosch process is highly optimized for large-scale production, where high capital costs are justified by large volumes of ammonia production during the plant lifetime. But the process is not suitable for small scales of production (< 1 ton/h) and cannot address all market needs.[2]

Low temperature (room temperature) electrochemical synthesis of green ammonia appears as a promising alternative to the green Haber-Bosch process. The reaction is performed in an electrochemical reactor at lower temperatures and pressures[3], without the need for costly components for heat recovery and for withstanding high pressures.[4] Operating at lower temperatures and milder pressures could help reduce capital costs, making the process relevant for smaller scales.[5] The electrochemical route has potential for decentralized production of ammonia[6] e.g., in vertical farming or at remote locations where transport costs make up a significant share of the total ammonia cost.

There have been several breakthroughs in this field, where ENRR was engineered to occur at near to 100% selectivity, and this field is no longer challenged by selectivity issues, as it historically was.[7] High selectivity of electrochemical synthesis of ammonia has been reported in both aqueous and non-aqueous media. Furthermore, new start-up companies intending to bring these technologies to the market have been established, and with these recent developments it is timely to assess electrochemical synthesis of ammonia for energy consumption and efficiency and benchmark it against the well-known Haber-Bosch Process. We also assess what were the most successful approaches these new technologies utilize.

However, until very recently ENRR was challenged by selectivity where proton or water reduction to hydrogen occurred predominantly as a side reaction.[8,9] Hydrogen evolution reaction (HER) is kinetically favoured, as it occurs in fewer steps than ENRR. Additionally, ENRR is often performed in aqueous media, where the solubility of N_2 is only about 0.7 mM at room temperatures and atmospheric pressure, while the concentration of the competing reactant that is involved in HER, i.e. water, is around 55 M, tens of thousands times more. The rates of electrochemical ammonia production in aqueous media are therefore often very low.

Because of low ENRR ammonia production rates, contamination can have a significant impact on an experimental result and lead to false positive measurements. For instance, ammonia was found present in the air, human breath, adsorbed within ion-exchange membranes as well as in nitrogen feed gas.[10] The presence of oxidized forms of nitrogen (NO_x), such as nitrate anions in catalyst materials, electrolytes for electrochemical cells, laboratory gloves and glassware and nitrogen oxides in nitrogen gas supplies or air, was also found problematic, because oxidized forms of N are more soluble in water and thermodynamically and kinetically easier to reduce to ammonia than dinitrogen, which highlights the need to properly clean the gases.[6,11,12] Some recent results reveal that some metal nitrides undergo chemical decomposition to produce ammonium instead of catalysing ENRR, which is yet another way of having a false positive measurement.[13]

To address the above-reported concerns, we first assessed published ENRR works for reliability before comparing them for energy consumption and efficiency. We used a methodology to assess the reliability of the articles established from rigorous ENRR protocols,[10] proposed by the research community to unambiguously confirm ENRR and stimulate the progress in the field.[12,13] The protocols proposed at least three different control experiments: i) control argon electrolysis experiments, ii) open-circuit potential experiments with N_2 gas, and iii) $^{15}N_2$ isotopic labelling experiments. If specific protocols did not follow these guidelines to confirm ENRR, some published research work can be hardly considered valid.[10,12] We assessed the published works by introducing our own reliability indicator table, where we defined two criteria that determine the likelihood for the ENRR work to be a false positive. Reliability indicator helped us focus the discussion of this review on the most promising catalysts, electrolytes, membranes, and cell designs & conditions. We calculated energy efficiency of most promising approaches and benchmarked them against the Haber-Bosch process.

Methods

A method to assess the reliability of ENRR works

Herein we evaluated the reliability of ENRR reports published from January 2019 to August 2022. The most reliable works were evaluated in terms of energy efficiency. We evaluated each study in terms of two criteria: experimental controls and ammonia production rate. The outputs

of this step allowed us to establish a reliability indicator table and calculate a reliability indicator to assess how likely the result was a false positive.

Experimental controls are a necessity to confirm the ENRR and to advance the state of the art of the ENRR field. We reviewed ENRR experimental protocols (SI section 1) to identify the requirements needed to unambiguously confirm the ENRR.

Based on the review of experimental protocols, the claim that ammonia stems from ENRR was very likely if: i) the amount of ammonia produced with $^{14}N_2$ is quantitatively reproducible with the $^{15}N_2$ experiments, ii) the gases have been adequately cleaned, and iii) the experiments were performed at least in triplicate and shown to be repeatable.

The production rate is a measure of the reliability of results. If the rates were low, it would have been difficult to discern between the ammonia stemming from contamination and actual production.[14] However, if ammonia production rates were high, the amount of produced ammonia would have been much higher than the contamination levels, which indicates a more reliable result.

The methodology we used to assess the reliability of ENRR articles was based on these requirements, as depicted in Fig. 1.

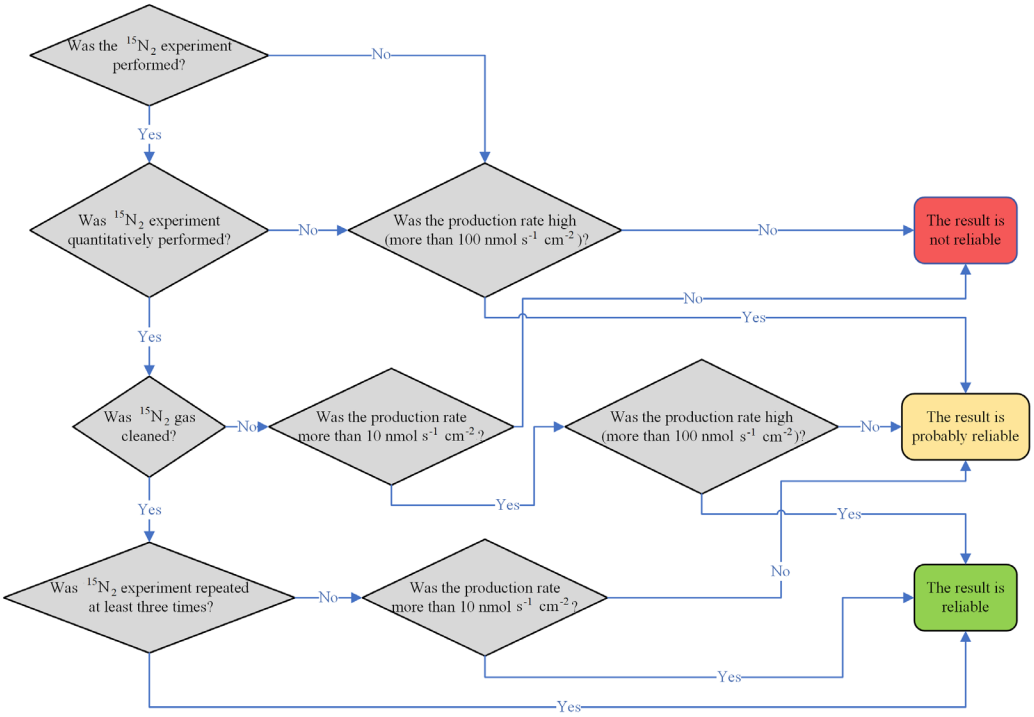

Figure 1 – Experimental protocol requirements to avoid false positive results and deliver reliable outputs: this flowchart is used to assess the articles and determine their reliability.

The experimental controls scoring. To evaluate the works based on the experimental control criterion, we have adopted the scale presented in Table 1, where the highest number defines the most reliable experiment. Here we put more weight on those experiments that cleaned gases and repeated the experiments than those that did not, as there is a smaller chance that the ammonia stemmed from a contamination of purified gas. For this purpose, we used a sigmoid-shaped function to score the intervals, as shown in Table 1. Here the plateau was at 25, for works that performed multiple 3 $^{15}N_2$ experiments with cleaned gases.

Table 1 – Sigmoid-shaped scored confidence intervals of different types of experiments performed in ENRR works.

Experimental control	Scale
No $^{15}N_2$ experiment	1
Qualitative $^{15}N_2$ experiment, without gas cleaning or repeating the experiment	2
Quantitative $^{15}N_2$ experiment, without gas cleaning or repeating the experiment	3
Quantitative $^{15}N_2$ experiment, with gas cleaning, but without repeating the experiment	10
Quantitative $^{15}N_2$ experiment, with gas cleaning and repeating the experiment	25

Ammonia production rate (J_{NH_3}) scoring. The minimum acceptable practical ammonia production rate for electrochemical ammonia synthesis was 100 nmol s^{-1} cm^{-2}.[15] In our evaluation of this criterion, we used the scale presented in Table 2. The scales are derived from Choi et al.'s work[14] where ammonia production rates are divided in 4 tiers. The scoring of the intervals follows a quasi-logarithmic scale covering more than 3 order of magnitudes, and it plateaus at 10. Here, the lowest production rate level (below 0.1 nmol s^{-1} cm^{-2}) has the lowest score of 1, while the highest has a score of 10. If production rates are higher than 100 nmol s^{-1} cm^{-2} ENRR works would be considered competitive with the Haber-Bosch process and therefore we score it high.

Table 2 – Quasi-logarithmic shaped scored intervals of ammonia production rate reported in various ENRR works.

Ammonia production rate	Scale
Ammonia production rate < 0.1 nmol s^{-1} cm^{-2}	1
0.1 < Ammonia production rate < 10 nmol s^{-1} cm^{-2}	2
10 < Ammonia production rate < 100 nmol s^{-1} cm^{-2}	4
Ammonia production rate > 100 nmol s^{-1} cm^{-2}	10

To determine the reliability of the process, we multiplied the scale values from Table 1 and Table 2 to calculate a new value, that we named the reliability indicator. The reliability indicator is presented as a matrix in Table 3. We defined three levels of confidence based on reliability indicator: red, yellow, and green, representing "not reliable", "probably reliable", and "reliable", respectively. The boundaries were carefully chosen as 10 and 25 to divide the articles into three levels of reliability. More specifically, we assign a high weight for a well-performed $^{15}N_2$ experimental control. For example, the first boundary index, 10, is the product of "quantitative $^{15}N_2$ experiment, with gas cleaning, but without repeating the experiment" and an unlikely practical production rate (J_{NH_3}< 0.1), which means even with a very low production rate and no repeatability, the result is probably reliable. The next boundary index is 25 because it results from a highly reliable $^{15}N_2$ experimental control that did the gas cleaning and repeated the experiments, however reporting a low production rate (J_{NH_3}< 0.1). Finally, we score 250 for a work with practically relevant production rate and highly reliable $^{15}N_2$ experimental control, that considered the gas cleaning and repeated the experiments.

Table 3 - Reliability indicator matrix – In this matrix, two intervals (10 and 25) were used to divide the reliability indicator into three levels: reliable, probably reliable, and not reliable. If the reliability indicator value is less than 10 the work falls within a "not reliable" interval and is marked with red colour. If the reliability indicator was between 10 and 25 the work falls within a "probably reliable" and is marked with yellow colour, and finally if the reliability indicator was greater than 25 the work falls within a "reliable" interval and is marked with green colour.

Reliability indicator		Ammonia production rate (nmol s^{-1} cm^{-2})			
		J_{NH_3}< 0.1	0.1 <J_{NH_3} <10	10 < J_{NH_3}< 100	J_{NH_3}>100
$^{15}N_2$ experimental controls	Scale	1	2	4	10

No $^{15}N_2$ experiment	1	1	2	4	10
Qualitative $^{15}N_2$ experiment, without gas cleaning or repeating the experiment	2	2	4	8	20
Quantitative $^{15}N_2$ experiment, without gas cleaning or repeating the experiment	3	3	6	12	30
Quantitative $^{15}N_2$ experiment, with gas cleaning, but without repeating the experiment	10	10	20	40	100
Quantitative $^{15}N_2$ experiment, with gas cleaning and repeating the experiment	25	25	50	100	250

Method to calculate the energy efficiency of ENRR works

Energy efficiency of ENNR. The energy efficiency of the ammonia synthesis process can be expressed as a power to fuel efficiency (η_{LHV}), which can be defined as:

$$\eta_{LHV} = \frac{LHV}{\Delta H_R} \quad (1)$$

where LHV is the lower heating value of ammonia (kJ/mol) and ΔH_R is the molar enthalpy of the reaction where fuel is synthesized (kJ/mol). In case of green ammonia, ΔH_R refers to the chemical reaction $\frac{1}{2}$ $N_2(g) + \frac{3}{2}$ $H_2O(l) \leftrightarrow NH_3(g) + \frac{3}{4}$ $O_2(g)$, where ΔH_R= 383 kJ/mol, which is calculated from the products and reactants standard enthalpy of formation,[16] as H_2 in green ammonia synthesis comes from water. The lower heating value (LHV) is the amount of energy released from burning 1 mol of fuel without recovery the latent heat of condensation of steam. LHV of ammonia is 317 kJ/mol[17] and by using Eq. (1) we can calculate, in case of green ammonia synthesis from water as a source of hydrogen, the maximum attainable thermodynamic energy efficiency as η_{LHV}= 82.77%. Practically, energy efficiency is calculated by dividing the LHV by the total energy input needed to synthesize ammonia, which includes the energy losses.

We calculated the energy needed to run the nitrogen electrolyser and used it as total energy input, meaning all energy efficiencies are overestimated. Electrical energy input to power up the nitrogen electrolyser is related to the working full cell voltage of an electrolyser, E_{cell}, which is defined as Eq. (2).

$$E_{\text{cell}} = E_{\text{ENRR}} - E_{\text{anode}} \quad (2)$$

where E_{anode} is the practically relevant potential at which water, hydrogen, or ethanol (depending on what is the source of the protons) gets oxidized. Eq. (2) does not contain any ohmic parasitic resistance (e.g. contact resistances, membrane resistance), and thus can be considered a lower limit for the operating voltage of a working device. E_{anode} is normally not reported; however, water oxidation potentials at different pH are readily available in the literature. For aqueous systems, we surveyed eight works and found the water oxidation potential (mean ± standard deviation) to be 1.6 ± 0.17 V vs. RHE (section 2, Table S1). For ethanol-based systems 0.4 V vs. RHE is used.[18] E_{ENRR} is the potential at which N_2 gets reduced to ammonia in a particular electrolyte, which is reported in ENRR works. E_{cell} calculated in Eq. (2) includes all the overpotentials and thus energy losses associated with the electrodes. The total electrical work used to power the electrolyser is given by Eq. (3):

$$W(\mathrm{NH_3}) = \frac{-nNFE_{\text{cell}}}{F.E.} \quad (3)$$

where $W(\mathrm{NH_3})$ is the electrical work (kJ/mol), n is number of moles of ammonia, N is the number of electrons transferred per molecule of ammonia (which is 3), F represents Faraday's constant, and $F.E.$ is Faraday efficiency. For aqueous systems the energy efficiency can be approximated as:

$$\eta_{\text{aq}} = \frac{LHV}{W(\mathrm{NH_3})} \quad (4)$$

Here $W(\mathrm{NH_3})$ in Eq. (4) is a proxy for the total energy input, since it does not account for heat (entropy) input (low at 25 °C), energy used to separate nitrogen from air, compress the gases and energy needed to separate clean liquid and anhydrous ammonia from the process. Of all the above-mentioned additional energy inputs, we anticipate the separation of pure ammonia being the largest omitted contribution affecting the energy efficiency. However, by using Eq. (4) we still get a practically relevant information in how the process stands against Haber-Bosch as energy input in Eq. (4) is the largest (around 80%)

For anhydrous systems we recognise the relevance of Eq. (4) for reporting energy efficiency of a given setup. However, when comparing aqueous and non-aqueous systems one needs to account for the energy input to produce the proton and electron source. Anhydrous systems are usually fuelled by hydrogen or ethanol, so the energy used to produce these chemicals should be considered when comparing the energy efficiency. For hydrogen as proton and electron

source, energy consumption can be calculated as energy used by alkaline electrolyser, where electrical work can be calculated with Eq. (5).

$$W(\mathrm{H_2}) = \frac{-nN(\mathrm{H_2})FE_{\mathrm{electrolyser}}}{F.E.} \quad (5)$$

Where $N(\mathrm{H_2})$ = 3 electrons (3/2 H_2 react with 1/2 N_2 to from 1 mol NH_3), and $E_{\mathrm{electrolyser}}$ is operating voltage of an alkaline electrolyser on a system level. Based on this equation, the energy needed to produce hydrogen is 707.56 kJ/mol NH_3 (see SI, section 4.1). The energy contribution from ethanol is estimated as 927.38 kJ/mol NH_3 (see SI, section 4.2).

For non-aqueous systems that used hydrogen gas or ethanol as a proton and electron source, the energy efficiency was calculated as described in Eq. (6) for H_2 and ethanol in Eq. (7).

$$\eta_{\mathrm{non-aq(H_2)}} = \frac{LHV}{W(\mathrm{NH_3})+W(\mathrm{H_2})} \quad (6)$$

$$\eta_{\mathrm{non-aq(EtOH)}} = \frac{LHV}{W(\mathrm{NH_3})+\frac{3}{4}\times LHV_{\mathrm{EtOH}}} \quad (7)$$

Here Eq. (3) was used to calculate $W(\mathrm{NH_3})$ and an estimate of E_{anode} in non-aqueous media was needed. In anhydrous systems where hydrogen was used at the anode, E_{anode} was set to 0.05 V vs. RHE.[19] For ethanol-based systems 0.4 V vs. RHE was used.[18] The real cell potential would be to some extent larger in a fully assembled electrochemical cell.[4] More reliable estimates for the electrical energy losses in a working device, need information from scaled up electrochemical stacks, which are not available as of today due to the TRL of this novel technology. In any case, the use of Eqs. (3)-(7) allows for a fair comparison of different ENNR systems as well as a preliminary benchmarking against Haber-Bosh.

Energy efficiency of conventional Haber-Bosch plants ranges from 36 to 62% depending on the age of the plant and the technology provider.[20] The energy efficiency of the green Haber-Bosch process that couples the hydrogen production from water electrolysis with the thermocatalytic step used in the Haber-Bosch process is reported as 56%.[16] We assumed ENRR must be run at least in this range of energy efficiencies to be competitive with Haber-Bosch. It is probably not realistic to expect energy efficiencies much higher than 60% in any ammonia-producing process, as the energy most intensive step in the Haber-Bosch process, which accounts for more than 90% of the energy use, is the hydrogen production where it proved very challenging to bring the energy cost down. Indeed, hydrogen production always occurs with inherent energy losses, whether it is produced by electrolysis or steam reforming of methane or coal.[21]

To evaluate energy efficiency, we used the intervals presented in Table 4. If a probably reliable/reliable ENRR work had $\eta < 20\%$, the work was not considered practically relevant, because less than 1 out of 5 Joules of total used energy goes in ammonia production. In such cases, most of the energy is used to generate heat or produce by-product hydrogen. If $20\% < \eta < 35\%$, the process was considered practically relevant in some applications where low capital cost might be more important than higher energy costs. The ENRR works in this range were identified promising, nonetheless they still need improvement. If the energy efficiency is in the range of $35\% < \eta < 60\%$, which was identified as the current range of efficiencies of Haber-Bosch ammonia plants, it was marked practically relevant. Finally, energy efficiencies higher than 60% were highly relevant and a future target not only for ENRR but also Haber-Bosch.

Table 4 – Classification of ENRR energy efficiency: the practically relevant of ENRR are classified into four different levels in terms of the energy efficiency

ENRR energy efficiency	Practically relevant level
$\eta < 20\%$	not practically relevant but still depends to target market
$20\% < \eta < 35\%$	probably practical relevant
$35\% < \eta < 60\%$	practically relevant
$\eta > 60\%$	highly relevant and future target

Results and discussion

The literature review included aqueous ENRR and non-aqueous ENRR works that performed $^{15}N_2$ experiments (Fig 1). We focused on identifying what seem to be promising research directions and to identify promising synergies between catalysts, cell designs, operating conditions and electrolyte. We then benchmarked the energy efficiency of these works against Haber-Bosch ammonia plants.

Successful approaches for achieving the high selectivity of the ENRR

Using the methodology outlined above we filtered out the results that have a high risk of being false positives (Section 3, SI). Having focused only on probably reliable and reliable works, we observe the selectivity of the electrochemical reaction measured through Faradaic efficiency spans from 5 to 99%, depending on the catalyst, electrolyte and the solvent (see Fig

2). Until recently, the major problem associated with ENRR was very low selectivity toward NH_3, where most of the electrons and protons were involved in HER thereby producing hydrogen instead of ammonia. The selectivity challenge has been solved for both non-aqueous and aqueous media, which both demonstrate high selectivity (Fig 2).

However, high selectivity of the reaction and high production rates was so far demonstrated only in non-aqueous, water-free, highly concentrated electrolytes with low proton concentration and a catalyst that strongly binds nitrogen. The non-aqueous media-based reports are presented in SI, Table S3. All non-aqueous media reports are based on lithium-mediated electrochemical nitrogen reduction reaction (Li-ENRR). Non-aqueous works are found in the right side of the plot (Fig 2), demonstrating much higher ammonia production rates than aqueous works, even if the Faradaic efficiency is in the same range of the aqueous works. This is in some part because the pressures of N_2 (up to 20 bar) are much higher than in aqueous works (mostly atmospheric pressure) and in some part attributed to the fact that N_2 solubility in aqueous solutions is lower than in non–aqueous electrolytes, such as ionic liquids.[22] Higher N_2 solubility in electrolytes results in larger adsorption of N_2 at active catalyst sites.[22] Back in 2017, Singh et al.[9] predicted that the selectivity challenge might be solved by reducing the proton concentration and using a catalyst that strongly binds nitrogen. They observed that NH_3 formation rate is zeroth order in the proton and electron concentration, while the H_2 formation rate is first order in both. Therefore, they concluded that a strategy for increasing the NH_3 selectivity could be to lower the accessibility of electrons, protons, or both. This would slow HER while the ammonia synthesis rate would be kept nearly the same. Based on this analysis, they proposed possible approaches to improve NH_3 selectivity might be in: i) decreasing the proton concentration in the electrolyte; ii) increasing the barrier for proton to transfer to catalyst surface in order to limit the proton transfer rate; iii) creating a thin insulating layer electrons must tunnel through or using photoabsorbers to supply a low flow of electrons in order to limit the electron transfer rate.[9] Indeed all successful works achieved high selectivity using one of the strategies explained above. Andersen et al.[23] demonstrated a stable operation of Li-ENRR with a potential cycling strategy, which enabled stable operation over several days. The Faradaic efficiency increased from 20% without cycling strategy to 37% with cycling strategy but not at a high yield rate (below 1 nmol s^{-1} cm^{-2}), at 10 bar pressure nitrogen. Cycling strategy essentially reduces the amount of protons adsorbed at the catalyst surface when the potential is not applied. Suryanto and coworkers[3] also implemented Li-ENRR for a reasonable

time frame. They mentioned that one factor limiting the performance and longevity of the Li-ENRR system is the chemical nature of the proton source participating in reaction, which is mostly ethanol, and it is used as a sacrificial material somewhat implying there is an optimal acidity of the electrolyte. Indeed, this has been known earlier both on a theoretical and experimental level.[24] Therefore, they introduced a phosphonium salt as a genuine recycling proton shuttle that was electrochemically stable as there was a minimal tendency for it to be oxidised or reduced at the electrodes and has an optimal acidity constant (pK_a around 4). They pressurized their cell to 19.5 bar of nitrogen, and this enabled a high ammonia production rate at 69% Faradaic efficiency in 20-hour experiments. Furthermore, Li et al.[25] showed that adding a small amount of oxygen to the feed gas had a positive effect on the process that significantly improved the Faradaic efficiency up to 78% at 0.6 to 0.8 mole % oxygen in 20 bar of nitrogen and improved the stability of the system.

Cai et al.[26] applied the strategy of keeping deposited lithium fresh by increasing electrolysis current to increase ammonia yield rate and Faradaic efficiency up to 39.5%. They demonstrated that Li-ENRR began with electrochemical deposition of lithium, followed by two chemical reactions of dinitrogen splitting and protonation. So, the only dominant electrochemical process was lithium plating; therefore, the generation speed of new lithium could be easily tuned by current. They also mentioned that fresh lithium could be obtained by retarding metallic lithium's passivation, which resulted from reaction between metallic lithium and electrolyte.

A breakthrough in Faradaic efficiency of up to 100% was recently achieved by Du and coworkers.[7] They investigated the role of electrolytes in Li-ENRR and presented a high Faradaic efficiency, approaching 100% at 15 bar nitrogen pressure. In this work, the electrolyte was high concentration imide-based lithium salt, making a compact ionic layering in the electrode-electrolyte interface. Several experiments were conducted to determine the optimum electrolyte type and concentration, as well as potential. $LiNTf_2$ was determined to be the best

electrolyte among LiOTf, $LiClO_4$ and $LiBF_4$, and FSI^-, with 2 M concentration at -0.55 V vs $Li^{0/+}_{app}$.

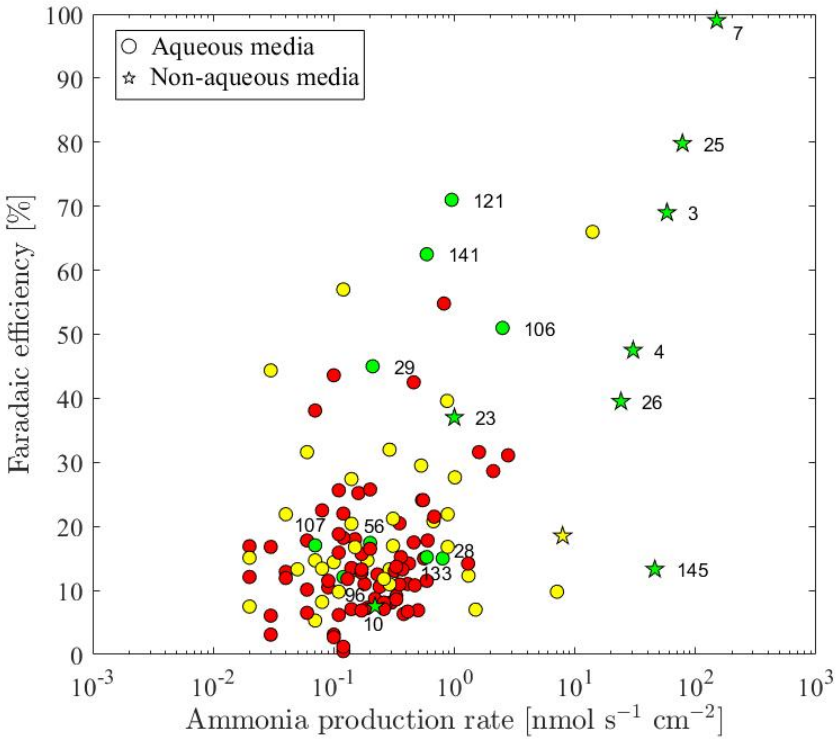

Figure 2- Reliability distribution of reviewed studies in terms of Faradaic efficiency – the green articles are reliable works, the yellow articles are probably reliable, and the red articles are non-reliable, assessed using the methodology depicted in Fig 1 and specified in Table 3. [3,4,10], [7,23,25–145]

The fully reliable aqueous works with Faradaic efficiency above 20% are summarized in Table 1. In terms of the reactor design, all four highly efficient and reliable aqueous media-based ENRR were conducted in a membrane-separated two-compartment cell under ambient conditions, in which the membrane mainly was proton exchange (Nafion 211,[29,141] Celgard,[121] Nafion 117[106]). The working electrode mainly was a carbon paper[29,121] or a carbon cloth[141] deposited with catalyst or fabricated by immobilizing the catalyst to a glassy carbon disc[106]. Indeed, gas diffusion electrodes (GDEs) can be used to overcome the diffusion limitations of gaseous reactants in electrochemical reactions, enabling intimate contact between the gas, electrolyte, and catalyst. With GDEs, the distance that gas must travel through the electrolyte to react at the catalyst surface is minimised, and the diffusion rate is increased compared to flooded electrodes in electrolytes. In non-aqueous works only Lazouski and coworkers[4] used stainless steel cloth-based (SSCs) support as cathode and anode support to overcome hydrogen and nitrogen gas diffusion limitation, respectively. They electrodeposited platinum onto the SSCs to be used as anode, as stainless steel is a poor hydrogen oxidation catalyst, and lithium

metal was plated in situ onto SSC substrate applied as cathode. Despite the high Faradaic efficiency of 47.5 at ambient conditions with these metal cloth-based supports, the cell potential was high 20-30 V, and the system was only stable for a short time. High voltages mainly arise from a very large electrical resistance of the non-aqueous electrolyte.

Table 1-Reliable aqueous media ENRR articles with high Faradaic efficiency (more than 20%)- All these works have a well performed $^{15}N_2$ experimental control that did the gas cleaning and repeated the experiments

No.	Catalyst	Electrolyte	FE%	Production rate (nmol s^{-1} cm^{-2})	Experimental control scale	Ammonia production rate scale	Reliability indicator	Ref.
1	B-COF/NC	0.1 M KOH	45	0.21	25	2	50	[29]
2	Fe-SAs/LCC/GC (Fe-O bond)	0.1 M KOH	51.0	2.51	25	2	50	[106]
3	B-COF/GO	10 M LiCl	71	0.95	25	2	50	[121]
4	WeSe2-x	12 m LiClO4	62.5	0.59	25	2	50	[141]

In terms of the catalyst three of these four aqueous ENRR are metal-free catalysts (numbers 1, 3, and 4 in Table 1).

In two of them, which were performed by Yan et al. group, the covalent organic framework-based materials (COF-based) were used as electrocatalyst.[29,121] Covalent organic frameworks are extended crystalline organic materials with unique architectures, high surface areas, and tuneable pore sizes.[146] On the other hand, their relatively low conductivity, which yields low charge carrier mobility,[146] could account for their high FE in ENRR; according to Singh et al. discussion,[9] limiting electron accessibility can improve NH_3 selectivity by surpassing the HER. Also, Zhao et al.[146] mentioned that for COF-based HER catalysts, the so far presented electrocatalytic performances are still lower than those for Pt-based systems and many other non-noble metal HER catalysts due to their poor conductivity. Furthermore, boron-rich covalent organic frameworks featuring strong Lewis acidity greatly promote the N_2 (as a weak Lewis base) adsorption.[29,147] DFT calculations combined with experiments performed by Yan et al. group demonstrated that electrochemical excitation of boron-rich COFs could facilitate the N_2 accessibility to catalyst (Eex-COF/NC) and achieve efficient ENRR. The electrolyte they used was 0.1 M KOH with a pH of 13, which this alkaline solvent with very few proton donors provides a situation to limit the access to protons and, consequently, suppress HER. Their work led to an efficient ENRR with high Faradaic efficiency of 45.43%.[29] In another

work by Yan et al. group,[121] covalent organic frameworks with abundant boron sites were uniformly grown on graphene oxide nanosheet substrate to achieve great exposure of active sites (B-COF/GO). They also applied salting-out effect in a highly concentrated pH-neutral electrolyte solution, which not only reduces proton accessibility but also water activity, which could be beneficial for the selectivity of ENRR according to Singh et al.[9]. Indeed, highly concentrated LiCl (12 M) was suggested by molecular dynamic (MD) simulation and verified by various in situ characterization, and finally confirmed by experiments results leading to a very high Faradaic efficiency of 71%.[121]

The third article that applied metal-free catalyst to implement ENRR was by Shen et al.[141]. Combining catalyst and electrolyte engineering in this work led to a highly efficient electrochemical nitrogen reduction system with a promising Faradaic efficiency of 62.5%. The catalyst that was used in this work was WSe_{2-x} nanosheet which was obtained from WSe_2 nanosheet annealed under a mixed Ar/H_2 atmosphere to create enriched Se vacancies verified by extensive characterizations. The free energy diagram of ENRR and HER on WSe_2 and WSe_{2-x} displayed that WSe_{2-x} exhibited a strong tendency for H_2O dissociation, which favoured the HER and retarded the ENRR; therefore, they adopted an electrolyte engineering strategy to suppress the HER by using water-in-salt electrolyte (WISE). To assess the role of electrolyte, they performed ENRR with WSe_{2-x} catalyst in two different electrolytes, diluted electrolyte (DE) 0.5 m $LiClO_4$ and WISE 12 m $LiClO_4$. The linear sweep voltammetry (LSV) curves of WSe_{2-x} in Ar and N_2 saturated DE and WISE showed that the current density difference between Ar and N_2 in WISE was larger than that in DE, which indicated that HER could be suppressed in WISE. Qualitative experiments also proved this by reaching high Faradaic efficiency of 62.5% in WISE compared to 11.8% in DE. Furthermore, the important role of catalyst engineering was experimentally proved by performing ENRR with WSe_2 in WISE, exhibiting 21.3% Faradaic efficiency, about three times lower than WSe_{2-x}.

Besides these three metal-free-based catalyst ENRR works, a metal-based catalyst ENRR work[106] showed an efficient reduction of nitrogen to ammonia with a high Faradaic efficiency of 51%. According to Skúlason and coworkers,[148] Fe, Mo, Ru, and Rh, placed on top of the volcano plot, are the most active metals in ENRR. However, these surfaces are probably saturated by H adatoms instead of N, resulting in pronounced competing HER and ENRR efficiency. Structural modification and catalyst engineering could help to increase the NH_3 selectivity of these metals. Since specific activity per metal atom increases with downsizing

metal particles, the size of a metal catalyst is a key factor determining the catalytic performance. It is possible to achieve the ultimate specific activity with single-atom catalysts (SACs), which contain atomically dispersed metal atoms in support materials.[149] Choi and coworkers[149] conducted DFT calculations on several SACs for ENRR. Specifically, they found that SACs exhibit a more positive free energy change of H adsorption (ΔG(*H)) than most metal surfaces, suggesting that HER can be suppressed and the ENRR selectivity could be dramatically improved. Based on their discussion, the efficient reduction of nitrogen to ammonia via a high Faradaic efficiency of 51% of Zhang et al.[106] could result from applying Fe-based SAC as electrocatalyst. In their work, a coordination of Fe-$(O\text{-}C_2)_4$ as active sites supported on nitrogen-free lignocellulose-derived carbon was used as electrocatalyst, immobilized on a glassy carbon electrode. In the ENRR experiment, 0.1 M KOH at 12.7 pH as electrolyte helped NH_3 selectivity with more suppression of HER.

Tables S2 and S3 show that a small fraction of works performed experimental controls in accordance with protocols (with experimental control scale number 25). Our evaluation made us realize that researchers should consider experimental protocols very seriously if they wish to stimulate progress and advance the state of the art of the field. The assessment of reliability of 117 articles reporting ENRR in aqueous media resulted with 34 publications being probably reliable and rated yellow, as presented in Table S1, and 9 publications rated green. The situation is much better for non-aqueous works, Table S2. Nevertheless, only 40% of ENRR works published during the last three and half years were assessed probably reliable or reliable (Fig. 2). This number would be much smaller if we divided reliable/probably reliable results with the total number of the works found in the literature (e.g. including those that did not perform $^{15}N_2$ experiments).

Energy efficiency of ENRR benchmarked against the Haber-Bosch Process

We further evaluated 52 reliable and probably reliable (aqueous + non-aqueous) works and compared them by energy efficiency, by relating the low heating value of ammonia and total electrical energy input to produce ammonia using ENRR. We state again the present analysis does not involve the energy cost to separate out clean, liquid anhydrous ammonia from water/organic solvent and to purify/compress the reaction gases.

Our analysis, as presented in Tables S4 and S5 and Fig 3, showed that the reliable/probably reliable ENRR reports have a maximum energy efficiency of 41%, which is comparable to current Haber-Bosch ammonia plants, with two of them practically relevant, as shown in Table

2, which are both aqueous media-based. Less than 20 percent of the reliable/probably reliable ENRR reports had energy efficiency between 20-35%. The others had less than 20% energy efficiency and need more improvements to be comparable with the Haber-Bosch process.

Table 2- ENRR articles with a practically relevant rated energy efficiency (more than 35%)- These two works among all aqueous and non- aqueous based media ENRR works are energy efficient ENRR, which both are aqueous based media

No.	Catalyst	Electrolyte	FE%	Potential (V vs RHE)	Production rate (nmol s^{-1} cm^{-2})	Reliability indicator	Energy efficiency	Ref.
1	Fe_{SA}/CNx	0.1 M KOH	57	0	0.12	20	39.02	[35]
2	B-COF/GO	10 M LiCl	71	-0.3	0.95	50	40.92	[121]

The first practically relevant article in Table 2 is a probably reliable work with a reliability indicator of 20. Despite this promising efficiency, the purity of $^{15}N_2$ gas employed in this work was not reported. However, it is mentioned in the article that the N_2 feed gas was pure without stating any method of purification. They repeated the $^{15}N_2$ experiment and reported standard deviation of calculated data.[35] The second one is one of the four reliable aqueous based-media ENRR works with high Faradaic efficiency explained from different points of view in the discussion above.[121] Both practically relevant works in terms of the energy efficiency in Table 2 are coming from the same research group.

As shown in Fig 3 and Table S5, the energy efficiency of non-aqueous media works, despite their high reliability and high production rates, were less than 20%, with a maximum of 15.1%. This was due to the high energy use to produce proton/electron sources (hydrogen/ethanol) but also due to the high cell potentials needed to keep Li-mediated ENRR running. In the SI (Section 6) we calculated the practical maximum energy efficiency for ammonia production from H_2 as a proton/electron source using lithium mediated ENRR as an approach. We obtained 24.2% based on *LHV*, by considering that waste heat cannot be recovered efficiently at such low temperatures. Approximately one third of the energy cost in Li-mediated ENRR goes to the production of proton/electron source and two thirds to the electrochemical reactor. In Haber-Bosch process the loop and the reactor consume very little energy, below 10%, while the largest energy consumption is on the side of hydrogen (proton/electron source) production. The high cell potential in Li-mediated ENRR was needed because Li seems to be consumed during the ENRR and needs to be constantly regenerated. Li is the most reductive metal and needs very negative potentials to be reduced/regenerated (-3.04 V vs. standard hydrogen electrode), which sets the minimum theoretical cell potential of Li regeneration at 3.04 V, not

including any energy losses. Overall, the results in Fig 2 showed electrochemical synthesis of ammonia advanced significantly during the last few years, however improvements are needed in terms of energy efficiency.

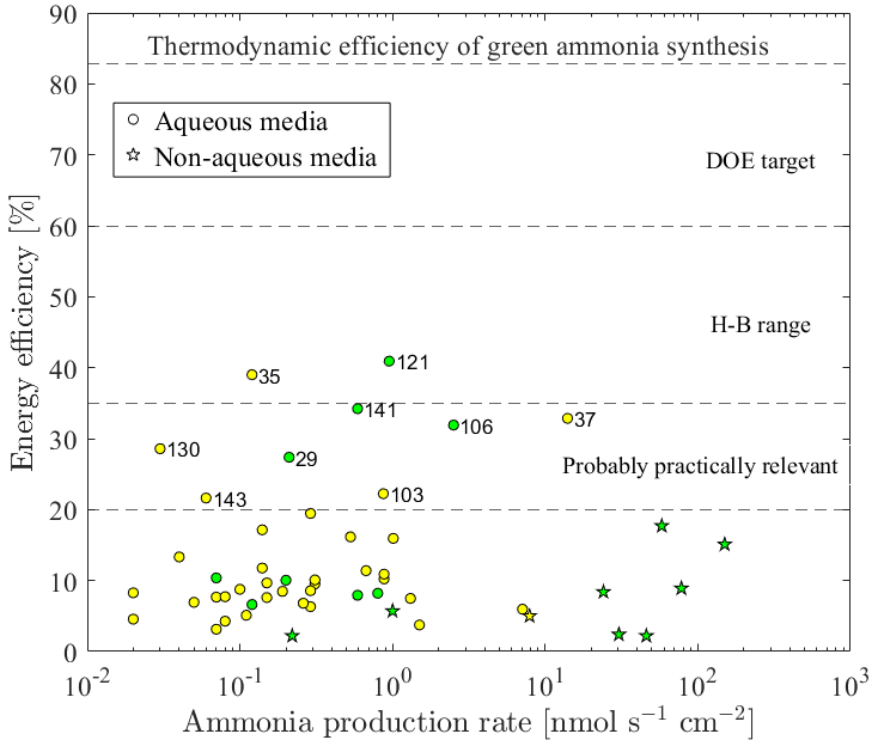

Figure 3- Energy efficiency of reviewed studies [3,4,7,10,23,25,26,28–30,35,37,40–42,45,46,55–58,60,71,72,79,85–87,89,92,96,98,100,102,103,106,107,112,115,120,121,123,125,126,130,131,133,134,140–143,145] *– There are four intervals between the lines: below 20% line is interval 1 which the articles are not practically relevant, between line one and two (20-35%) is interval 2 that is probably practically relevant, between line two and three (35-60%) represent interval 3 that are practically relevant, and above 60% is interval 4 that is goal for all processes including Haber-Bosch (H-B). The fourth line is the thermodynamic efficiency of green ammonia synthesis calculated based on the low heating value of ammonia. Colour codes are adopted from previous section, where yellow is probably reliable and green reliable ENRR work.*

Conclusions

The evaluation of the non-aqueous works revealed that the most promising approach to achieve high selectivity and production rates of ammonia in electrochemical ammonia synthesis was: i) using electroplated Li metal at the cathode; ii) non-aqueous electrolyte with an optimal Li salt and proton concentration and iii) higher operating pressure of nitrogen (up to 20 bar).

Successful approaches in aqueous media involved highly selective catalyst materials, electrolytes with low concentrations of protons or lower activity of water using water-in-salt

electrolytes and use of two compartment reactors separated by a membrane that favours the adsorption of nitrogen.

The evaluation of works in terms of their energy efficiency, reveals there are aqueous ENRR works that can achieve energy efficiency of up to 41%, and get ammonia dissolved in water, which makes them practically relevant and in Haber-Bosch range. But these energy efficiencies are lower than of state-of-art green ammonia plants (56%), which produce clean liquid ammonia. The energy efficiency of reliable non-aqueous works is less than 20% and here the product is ammonia dissolved in organic solvent. Lower energy efficiency is mainly related to very high cell potentials that are needed to constantly regenerate lithium metal, which ultimately increase the energy consumption of the electrochemical reactor. Thus, higher energy efficiencies must be achieved using catalysts beyond lithium.

Finally, during the last three and half years, in this rapidly advancing field, an admirable 40% of published works that performed $^{15}N_2$ experiments were assessed reliable or probably reliable, according to our strict methodology. Other works were assessed non-reliable due to the low quality of control experiments and this needs to be improved in the future to help advance the state of the art faster.

Acknowledgement

This work was supported by. 1) Horizon 2020 project, Grant agreement 101022738, funded under SOCIETAL CHALLENGES - Secure, clean and efficient energy and 2) Independent Research Fund Denmark, case number 0217-00234B. We acknowledge comments received from Dr. Egill Skúlason, University of Iceland, during the preparation of the manuscript.

Author contributions

Conception by ED and FR.
Data collection FR.
Data analysis and interpretation by all.
Drafting the article by all.
Critical revision of the article by all.
Final approval of the version to be published by ED.

Data availability

Upon request to the corresponding author.

Competing interests

The authors declare no competing interests.

References

1. Lin, B., Wiesner, T. & Malmali, M. Performance of a Small-Scale Haber Process: A Techno-Economic Analysis. *ACS Sustain. Chem. Eng.* **8**, 15517–15531 (2020).
2. Rouwenhorst, K. H. R., Van der Ham, A. G. J., Mul, G. & Kersten, S. R. A. Islanded ammonia power systems: Technology review & conceptual process design. *Renew. Sustain. Energy Rev.* **114**, 109339 (2019).
3. Suryanto, B. H. R. *et al.* Nitrogen reduction to ammonia at high efficiency and rates based on a phosphonium proton shuttle. *Science* **372**, 1187–1191 (2021).
4. Lazouski, N., Chung, M., Williams, K., Gala, M. L. & Manthiram, K. Non-aqueous gas diffusion electrodes for rapid ammonia synthesis from nitrogen and water-splitting-derived hydrogen. *Nat. Catal.* **3**, 463–469 (2020).
5. Ravi, M. & Makepeace, J. W. Facilitating green ammonia manufacture under milder conditions: what do heterogeneous catalyst formulations have to offer? *Chem. Sci.* **13**, 890–908.
6. Suryanto, B. H. R. *et al.* Challenges and prospects in the catalysis of electroreduction of nitrogen to ammonia. *Nat. Catal.* **2**, 290–296 (2019).
7. Du, H.-L. *et al.* Electroreduction of nitrogen at almost 100% current-to-ammonia efficiency. *Nature* (2022) doi:10.1038/s41586-022-05108-y.
8. Dražević, E. & Skúlason, E. Are There Any Overlooked Catalysts for Electrochemical NH3 Synthesis—New Insights from Analysis of Thermochemical Data. *iScience* **23**, 101803 (2020).
9. Singh, A. R. *et al.* Electrochemical Ammonia Synthesis—The Selectivity Challenge. *ACS Catal.* **7**, 706–709 (2017).
10. Andersen, S. Z. *et al.* A rigorous electrochemical ammonia synthesis protocol with quantitative isotope measurements. *Nature* **570**, 504–508 (2019).
11. Choi, J. *et al.* Electroreduction of Nitrates, Nitrites, and Gaseous Nitrogen Oxides: A Potential Source of Ammonia in Dinitrogen Reduction Studies. *ACS Energy Lett.* **5**, 2095–2097 (2020).

12. Li, L., Tang, C., Yao, D., Zheng, Y. & Qiao, S.-Z. Electrochemical Nitrogen Reduction: Identification and Elimination of Contamination in Electrolyte. *ACS Energy Lett.* **4**, 2111–2116 (2019).
13. MacLaughlin, C. Role for Standardization in Electrocatalytic Ammonia Synthesis: A Conversation with Leo Liu, Lauren Greenlee, and Douglas MacFarlane. *ACS Energy Lett.* **4**, 1432–1436 (2019).
14. Choi, J. *et al.* Identification and elimination of false positives in electrochemical nitrogen reduction studies. *Nat. Commun.* **11**, 5546 (2020).
15. Giddey, S., Badwal, S. P. S. & Kulkarni, A. Review of electrochemical ammonia production technologies and materials. *Int. J. Hydrog. Energy* **38**, 14576–14594 (2013).
16. Martín, A. J., Shinagawa, T. & Pérez-Ramírez, J. Electrocatalytic Reduction of Nitrogen: From Haber-Bosch to Ammonia Artificial Leaf. *Chem* **5**, 263–283 (2019).
17. Informatics, N. O. of D. and. NIST Chemistry WebBook. https://webbook.nist.gov/chemistry/ doi:10.18434/T4D303.
18. Mukouyama, Y., Iida, K. & Kuge, T. Electrooxidation of Ethanol on Pt in the Absence of Water. *Electrochemistry* **88**, 178–184 (2020).
19. Durst, J., Simon, C., Hasché, F. & Gasteiger, H. A. Hydrogen Oxidation and Evolution Reaction Kinetics on Carbon Supported Pt, Ir, Rh, and Pd Electrocatalysts in Acidic Media. *J. Electrochem. Soc.* **162**, F190 (2014).
20. Smith, C., K. Hill, A. & Torrente-Murciano, L. Current and future role of Haber–Bosch ammonia in a carbon-free energy landscape. *Energy Environ. Sci.* **13**, 331–344 (2020).
21. Morgan, E. R., Manwell, J. F. & McGowan, J. G. Sustainable Ammonia Production from U.S. Offshore Wind Farms: A Techno-Economic Review. *ACS Sustain. Chem. Eng.* **5**, 9554–9567 (2017).
22. Zhao, R. *et al.* Recent progress in the electrochemical ammonia synthesis under ambient conditions. *EnergyChem* **1**, 100011 (2019).
23. Andersen, S. Z. *et al.* Increasing stability, efficiency, and fundamental understanding of lithium-mediated electrochemical nitrogen reduction. *Energy Environ. Sci.* **13**, 4291–4300 (2020).
24. Chalkley, M. J., Del Castillo, T. J., Matson, B. D. & Peters, J. C. Fe-Mediated Nitrogen Fixation with a Metallocene Mediator: Exploring pKa Effects and Demonstrating Electrocatalysis. *J. Am. Chem. Soc.* **140**, 6122–6129 (2018).

25. Li, K. *et al.* Enhancement of lithium-mediated ammonia synthesis by addition of oxygen. *Science* **374**, 1593–1597 (2021).
26. Cai, X. *et al.* Lithium-mediated electrochemical nitrogen reduction: Mechanistic insights to enhance performance. *iScience* **24**, 103105 (2021).
27. Zhang, L., Ding, L.-X., Chen, G.-F., Yang, X. & Wang, H. Ammonia Synthesis Under Ambient Conditions: Selective Electroreduction of Dinitrogen to Ammonia on Black Phosphorus Nanosheets. *Angew. Chem.* **131**, 2638–2642 (2019).
28. Liu, Y.-T., Li, D., Yu, J. & Ding, B. Stable Confinement of Black Phosphorus Quantum Dots on Black Tin Oxide Nanotubes: A Robust, Double-Active Electrocatalyst toward Efficient Nitrogen Fixation. *Angew. Chem. Int. Ed.* **58**, 16439–16444 (2019).
29. Liu, S. *et al.* Facilitating nitrogen accessibility to boron-rich covalent organic frameworks via electrochemical excitation for efficient nitrogen fixation. *Nat. Commun.* **10**, 3898 (2019).
30. Liu, Y. *et al.* Dramatically Enhanced Ambient Ammonia Electrosynthesis Performance by In-Operando Created Li–S Interactions on MoS2 Electrocatalyst. *Adv. Energy Mater.* **9**, 1803935 (2019).
31. Wang, X., Wang, J., Li, Y. & Chu, K. Nitrogen-Doped NiO Nanosheet Array for Boosted Electrocatalytic N2 Reduction. *ChemCatChem* **11**, 4529–4536 (2019).
32. Kang, S. *et al.* Plasma-etching enhanced titanium oxynitride active phase with high oxygen content for ambient electrosynthesis of ammonia. *Electrochem. Commun.* **100**, 90–95 (2019).
33. Han, L. *et al.* Atomically Dispersed Molybdenum Catalysts for Efficient Ambient Nitrogen Fixation. *Angew. Chem.* **131**, 2343–2347 (2019).
34. Cong, L., Yu, Z., Liu, F. & Huang, W. Electrochemical synthesis of ammonia from N 2 and H 2 O using a typical non-noble metal carbon-based catalyst under ambient conditions. *Catal. Sci. Technol.* **9**, 1208–1214 (2019).
35. Wang, M. *et al.* Over 56.55% Faradaic efficiency of ambient ammonia synthesis enabled by positively shifting the reaction potential. *Nat. Commun.* **10**, 341 (2019).
36. Qin, Q. *et al.* Enhanced Electrocatalytic N2 Reduction via Partial Anion Substitution in Titanium Oxide–Carbon Composites. *Angew. Chem. Int. Ed.* **58**, 13101–13106 (2019).
37. Hao, Y.-C. *et al.* Promoting nitrogen electroreduction to ammonia with bismuth nanocrystals and potassium cations in water. *Nat. Catal.* **2**, 448–456 (2019).

38. Ahmed, M. I. *et al.* Metal–Sulfur Linkages Achieved by Organic Tethering of Ruthenium Nanocrystals for Enhanced Electrochemical Nitrogen Reduction. *Angew. Chem. Int. Ed.* **59**, 21465–21469 (2020).
39. Li, Y., Liu, Y., Wang, J., Guo, Y. & Chu, K. Plasma-engineered NiO nanosheets with enriched oxygen vacancies for enhanced electrocatalytic nitrogen fixation. *Inorg. Chem. Front.* **7**, 455–463 (2020).
40. Chu, K., Cheng, Y., Li, Q., Liu, Y. & Tian, Y. Fe-doping induced morphological changes, oxygen vacancies and Ce3+–Ce3+ pairs in CeO2 for promoting electrocatalytic nitrogen fixation. *J. Mater. Chem. A* **8**, 5865–5873 (2020).
41. Chu, K., Liu, Y., Cheng, Y. & Li, Q. Synergistic boron-dopants and boron-induced oxygen vacancies in MnO2 nanosheets to promote electrocatalytic nitrogen reduction. *J. Mater. Chem. A* **8**, 5200–5208 (2020).
42. Lai, F. *et al.* Oxygen vacancy engineering in spinel-structured nanosheet wrapped hollow polyhedra for electrochemical nitrogen fixation under ambient conditions. *J. Mater. Chem. A* **8**, 1652–1659 (2020).
43. Tong, W. *et al.* Crystal-Phase-Engineered PdCu Electrocatalyst for Enhanced Ammonia Synthesis. *Angew. Chem. Int. Ed.* **59**, 2649–2653 (2020).
44. Wu, X. *et al.* Chemically coupled NiCoS/C nanocages as efficient electrocatalysts for nitrogen reduction reactions. *J. Mater. Chem. A* **8**, 543–547 (2020).
45. Fang, W. *et al.* Hydrophilic engineering of VOx-based nanosheets for ambient electrochemical ammonia synthesis at neutral pH. *J. Mater. Chem. A* **8**, 5913–5918 (2020).
46. Luo, Y.-X., Qiu, W.-B., Liang, R.-P., Xia, X.-H. & Qiu, J.-D. Mo-Doped FeP Nanospheres for Artificial Nitrogen Fixation. *ACS Appl. Mater. Interfaces* **12**, 17452–17458 (2020).
47. Liu, Y. *et al.* A Highly Efficient Metal-Free Electrocatalyst of F-Doped Porous Carbon toward N2 Electroreduction. *Adv. Mater.* **32**, 1907690 (2020).
48. Li, J. *et al.* Accelerated Dinitrogen Electroreduction to Ammonia via Interfacial Polarization Triggered by Single-Atom Protrusions. *Chem* **6**, 885–901 (2020).
49. Gao, J. *et al.* Enabling electrochemical conversion of N2 to NH3 under ambient conditions by a CoP3 nanoneedle array. *J. Mater. Chem. A* **8**, 17956–17959 (2020).

50. Li, Q., Cheng, Y., Li, X., Guo, Y. & Chu, K. ZrB2 as an earth-abundant metal diboride catalyst for electroreduction of dinitrogen to ammonia. *Chem. Commun.* **56**, 13009–13012 (2020).
51. Yang, X. *et al.* Insights into the role of cation vacancy for significantly enhanced electrochemical nitrogen reduction. *Appl. Catal. B Environ.* **264**, 118477 (2020).
52. Wang, P., Li, Q., Cheng, Y. & Chu, K. In2O3 nanoparticle-reduced graphene oxide hybrid for electrocatalytic nitrogen fixation: Computational and experimental studies. *J. Mater. Sci.* **55**, 4624–4632 (2020).
53. Xu, X., Sun, B., Liang, Z., Cui, H. & Tian, J. High-Performance Electrocatalytic Conversion of N2 to NH3 Using 1T-MoS2 Anchored on Ti3C2 MXene under Ambient Conditions. *ACS Appl. Mater. Interfaces* **12**, 26060–26067 (2020).
54. Chu, K., Liu, Y., Li, Y., Guo, Y. & Tian, Y. Two-dimensional (2D)/2D Interface Engineering of a MoS_2/C_3N_4 Heterostructure for Promoted Electrocatalytic Nitrogen Fixation. *ACS Appl. Mater. Interfaces* **12**, 7081–7090 (2020).
55. Lai, F. *et al.* Refining Energy Levels in ReS2 Nanosheets by Low-Valent Transition-Metal Doping for Dual-Boosted Electrochemical Ammonia/Hydrogen Production. *Adv. Funct. Mater.* **30**, 1907376 (2020).
56. Fu, Y. *et al.* Dual-metal-driven Selective Pathway of Nitrogen Reduction in Orderly Atomic-hybridized Re2MnS6 Ultrathin Nanosheets. *Nano Lett.* **20**, 4960–4967 (2020).
57. Chu, K., Li, Q., Cheng, Y. & Liu, Y. Efficient Electrocatalytic Nitrogen Fixation on FeMoO4 Nanorods. *ACS Appl. Mater. Interfaces* **12**, 11789–11796 (2020).
58. Wang, H.-B. *et al.* Bionic Design of a Mo(IV)-Doped FeS2 Catalyst for Electroreduction of Dinitrogen to Ammonia. *ACS Catal.* **10**, 4914–4921 (2020).
59. Zhang, N. *et al.* Surface-Regulated Rhodium–Antimony Nanorods for Nitrogen Fixation. *Angew. Chem. Int. Ed.* **59**, 8066–8071 (2020).
60. Yang, C. *et al.* A Generalized Surface Chalcogenation Strategy for Boosting the Electrochemical N2 Fixation of Metal Nanocrystals. *Adv. Mater.* **32**, 2001267 (2020).
61. Yang, X. *et al.* Low-Coordinate Step Atoms via Plasma-Assisted Calcinations to Enhance Electrochemical Reduction of Nitrogen to Ammonia. *Small* **16**, 2000421 (2020).
62. Lv, X.-W. *et al.* ZIF-supported AuCu nanoalloy for ammonia electrosynthesis from nitrogen and thin air. *J. Mater. Chem. A* **8**, 8868–8874 (2020).

63. Chen, T., Liu, S., Ying, H., Li, Z. & Hao, J. Reactive Ionic Liquid Enables the Construction of 3D Rh Particles with Nanowire Subunits for Electrocatalytic Nitrogen Reduction. *Chem. – Asian J.* **15**, 1081–1087 (2020).
64. Guo, C. *et al.* Fe-doped Ni2P nanosheets with porous structure for electroreduction of nitrogen to ammonia under ambient conditions. *Appl. Catal. B Environ.* **263**, 118296 (2020).
65. Ma, M. *et al.* Tuning electronic structure of PdZn nanocatalyst via acid-etching strategy for highly selective and stable electrolytic nitrogen fixation under ambient conditions. *Appl. Catal. B Environ.* **265**, 118568 (2020).
66. Xu, W. *et al.* Nanoporous Palladium Hydride for Electrocatalytic N2 Reduction under Ambient Conditions. *Angew. Chem. Int. Ed.* **59**, 3511–3516 (2020).
67. Hao, R. *et al.* Efficient Electrochemical Nitrogen Fixation over Isolated Pt Sites. *Small* **16**, 2000015 (2020).
68. Zhao, X. *et al.* BCN-Encapsulated Nano-nickel Synergistically Promotes Ambient Electrochemical Dinitrogen Reduction. *ACS Appl. Mater. Interfaces* **12**, 31419–31430 (2020).
69. Zhao, H. *et al.* High-performance nitrogen electroreduction at low overpotential by introducing Pb to Pd nanosponges. *Appl. Catal. B Environ.* **265**, 118481 (2020).
70. Jin, M. *et al.* Efficient electrochemical N2 fixation by doped-oxygen-induced phosphorus vacancy defects on copper phosphide nanosheets. *J. Mater. Chem. A* **8**, 5936–5942 (2020).
71. Chen, Y. *et al.* Highly Productive Electrosynthesis of Ammonia by Admolecule-Targeting Single Ag Sites. *ACS Nano* **14**, 6938–6946 (2020).
72. Zhao, S. *et al.* An oxygen vacancy-rich two-dimensional Au/TiO2 hybrid for synergistically enhanced electrochemical N2 activation and reduction. *J. Mater. Chem. A* **8**, 6586–6596 (2020).
73. Li, H., Li, T.-T., Qian, J., Mei, Y. & Zheng, Y.-Q. CuCo2S4 integrated multiwalled carbon nanotube as high-performance electrocatalyst for electroreduction of nitrogen to ammonia. *Int. J. Hydrog. Energy* **45**, 14640–14647 (2020).
74. Wang, C., Gao, J., Zhao, J.-G., Yan, D.-J. & Zhu, X.-D. Synergistically Coupling Black Phosphorus Quantum Dots with MnO2 Nanosheets for Efficient Electrochemical Nitrogen Reduction Under Ambient Conditions. *Small* **16**, 1907091 (2020).

75. Lin, Y. *et al.* Sulfur Atomically Doped Bismuth Nanobelt Driven by Electrochemical Self-Reconstruction for Boosted Electrocatalysis. *J. Phys. Chem. Lett.* **11**, 1746–1752 (2020).
76. Qiu, Y. *et al.* Multi-yolk–shell bismuth@porous carbon as a highly efficient electrocatalyst for artificial N2 fixation under ambient conditions. *Inorg. Chem. Front.* **7**, 2006–2016 (2020).
77. Liu, Y. *et al.* Electrocatalytic production of ammonia: Biomimetic electrode–electrolyte design for efficient electrocatalytic nitrogen fixation under ambient conditions. *Appl. Catal. B Environ.* **271**, 118919 (2020).
78. Wang, J. *et al.* A General Strategy to Glassy M-Te (M = Ru, Rh, Ir) Porous Nanorods for Efficient Electrochemical N2 Fixation. *Adv. Mater.* **32**, 1907112 (2020).
79. Chu, K., Wang, J., Liu, Y., Li, Q. & Guo, Y. Mo-doped SnS2 with enriched S-vacancies for highly efficient electrocatalytic N2 reduction: the critical role of the Mo–Sn–Sn trimer. *J. Mater. Chem. A* **8**, 7117–7124 (2020).
80. Zhang, M. *et al.* Reduced graphene oxides with engineered defects enable efficient electrochemical reduction of dinitrogen to ammonia in wide pH range. *Nano Energy* **68**, 104323 (2020).
81. Peng, G. *et al.* Nitrogen-Defective Polymeric Carbon Nitride Nanolayer Enabled Efficient Electrocatalytic Nitrogen Reduction with High Faradaic Efficiency. *Nano Lett.* **20**, 2879–2885 (2020).
82. Xiao, S., Luo, F., Hu, H. & Yang, Z. Boron and nitrogen dual-doped carbon nanospheres for efficient electrochemical reduction of N2 to NH3. *Chem. Commun.* **56**, 446–449 (2020).
83. Liu, Z. *et al.* Defective Carbon-Doped Boron Nitride Nanosheets for Highly Efficient Electrocatalytic Conversion of N2 to NH3. *ACS Sustain. Chem. Eng.* **8**, 5278–5286 (2020).
84. Zhang, J. *et al.* Confinement of Intermediates in Blue TiO2 Nanotube Arrays Boosts Reaction Rate of Nitrogen Electrocatalysis. *ChemCatChem* **12**, 2760–2767 (2020).
85. Guo, Y. *et al.* Highly Efficient Electrochemical Reduction of Nitrogen to Ammonia on Surface Termination Modified Ti3C2Tx MXene Nanosheets. *ACS Nano* **14**, 9089–9097 (2020).

86. Luo, S. *et al.* Long-term electrocatalytic N 2 fixation by MOF-derived Y-stabilized ZrO 2 : insight into the deactivation mechanism. *J. Mater. Chem. A* **8**, 5647–5654 (2020).
87. Jin, Z. *et al.* Rational Design of Hydroxyl-Rich Ti3C2Tx MXene Quantum Dots for High-Performance Electrochemical N2 Reduction. *Adv. Energy Mater.* **10**, 2000797 (2020).
88. Nan, H., Liu, Y., Li, Q., Shen, P. & Chu, K. A Janus antimony sulfide catalyst for highly selective N2 electroreduction. *Chem. Commun.* **56**, 10345–10348 (2020).
89. Liu, Y., Luo, Y., Li, Q., Wang, J. & Chu, K. Bimetallic MnMoO4 with dual-active-centers for highly efficient electrochemical N2 fixation. *Chem. Commun.* **56**, 10227–10230 (2020).
90. Shen, P., Liu, Y., Li, Q. & Chu, K. FeVO4 porous nanorods for electrochemical nitrogen reduction: contribution of the Fe2c–V2c dimer as a dual electron-donation center. *Chem. Commun.* **56**, 10505–10508 (2020).
91. Cheng, Y., Nan, H., Li, Q., Luo, Y. & Chu, K. A Rare-Earth Samarium Oxide Catalyst for Electrocatalytic Nitrogen Reduction to Ammonia. *ACS Sustain. Chem. Eng.* **8**, 13908–13914 (2020).
92. Tian, Y. *et al.* A spinel ferrite catalyst for efficient electroreduction of dinitrogen to ammonia. *Dalton Trans.* **49**, 12559–12564 (2020).
93. Su, H. *et al.* Single Atoms of Iron on MoS2 Nanosheets for N2 Electroreduction into Ammonia. *Angew. Chem. Int. Ed.* **59**, 20411–20416 (2020).
94. Xu, X. *et al.* 1 T-phase molybdenum sulfide nanodots enable efficient electrocatalytic nitrogen fixation under ambient conditions. *Appl. Catal. B Environ.* **272**, 118984 (2020).
95. Ma, Y. *et al.* Synergizing Mo Single Atoms and Mo2C Nanoparticles on CNTs Synchronizes Selectivity and Activity of Electrocatalytic N2 Reduction to Ammonia. *Adv. Mater.* **32**, 2002177 (2020).
96. Chu, K. *et al.* Multi-functional Mo-doping in MnO2 nanoflowers toward efficient and robust electrocatalytic nitrogen fixation. *Appl. Catal. B Environ.* **264**, 118525 (2020).
97. Wang, H. *et al.* Exfoliated metallic niobium disulfate nanosheets for enhanced electrochemical ammonia synthesis and Zn-N2 battery. *Appl. Catal. B Environ.* **270**, 118892 (2020).
98. Zhang, L. *et al.* A Janus Fe-SnO2 Catalyst that Enables Bifunctional Electrochemical Nitrogen Fixation. *Angew. Chem.* **132**, 10980–10985 (2020).

99. Wang, S. *et al.* Identifying the Active Site on Graphene Oxide Nanosheets for Ambient Electrocatalytic Nitrogen Reduction. *Inorg. Chem.* **59**, 11108–11112 (2020).
100. Liu, B. *et al.* Nanostructured and Boron-Doped Diamond as an Electrocatalyst for Nitrogen Fixation. *ACS Energy Lett.* **5**, 2590–2596 (2020).
101. Ye, W. *et al.* Fe, Mo–N/C Hollow Porous Nitrogen-Doped Carbon Nanorods as an Effective Electrocatalyst for N2 Reduction Reaction. *ACS Sustain. Chem. Eng.* **8**, 15946–15952 (2020).
102. Zhang, S. *et al.* Laser Irradiation in Liquid to Release Cobalt Single-Atom Sites for Efficient Electrocatalytic N2 Reduction. *ACS Appl. Energy Mater.* **3**, 6079–6086 (2020).
103. Yang, H. *et al.* Achieving High Activity and Selectivity of Nitrogen Reduction via Fe–N3 Coordination on Iron Single-Atom Electrocatalysts at Ambient Conditions. *ACS Sustain. Chem. Eng.* **8**, 12809–12816 (2020).
104. Peng, W. *et al.* Spontaneous Atomic Ruthenium Doping in Mo2CTX MXene Defects Enhances Electrocatalytic Activity for the Nitrogen Reduction Reaction. *Adv. Energy Mater.* **10**, 2001364 (2020).
105. Li, W. *et al.* Bimetal–MOF nanosheets as efficient bifunctional electrocatalysts for oxygen evolution and nitrogen reduction reaction. *J. Mater. Chem. A* **8**, 3658–3666 (2020).
106. Zhang, S. *et al.* Electrocatalytically Active Fe-(O-C2)4 Single-Atom Sites for Efficient Reduction of Nitrogen to Ammonia. *Angew. Chem. Int. Ed.* **59**, 13423–13429 (2020).
107. Yuan, M. *et al.* Support effect boosting the electrocatalytic N2 reduction activity of Ni2P/N,P-codoped carbon nanosheet hybrids. *J. Mater. Chem. A* **8**, 2691–2700 (2020).
108. Lai, F. *et al.* N2 Electroreduction to NH3 by Selenium Vacancy-Rich ReSe2 Catalysis at an Abrupt Interface. *Angew. Chem. Int. Ed.* **59**, 13320–13327 (2020).
109. Wang, P., Ji, Y., Shao, Q., Li, Y. & Huang, X. Core@shell structured Au@SnO2 nanoparticles with improved N2 adsorption/activation and electrical conductivity for efficient N2 fixation. *Sci. Bull.* **65**, 350–358 (2020).
110. Ling, Y. *et al.* Strain induced rich planar defects in heterogeneous WS2/WO2 enable efficient nitrogen fixation at low overpotential. *J. Mater. Chem. A* **8**, 12996–13003 (2020).

111. Xia, L. *et al.* Engineering Abundant Edge Sites of Bismuth Nanosheets toward Superior Ambient Electrocatalytic Nitrogen Reduction via Topotactic Transformation. *ACS Sustain. Chem. Eng.* **8**, 2735–2741 (2020).
112. Wang, Y. *et al.* Self-supported NbSe2 nanosheet arrays for highly efficient ammonia electrosynthesis under ambient conditions. *J. Catal.* **381**, 78–83 (2020).
113. Zhang, J. *et al.* Adsorbing and Activating N2 on Heterogeneous Au–Fe3O4 Nanoparticles for N2 Fixation. *Adv. Funct. Mater.* **30**, 1906579 (2020).
114. Wang, T. *et al.* Commercial indium-tin oxide glass: A catalyst electrode for efficient N2 reduction at ambient conditions. *Chin. J. Catal.* **42**, 1024–1029 (2021).
115. Lin, G. *et al.* Intrinsic Electron Localization of Metastable MoS $_2$ Boosts Electrocatalytic Nitrogen Reduction to Ammonia. *Adv. Mater.* **33**, 2007509 (2021).
116. Wang, P., Nong, W., Li, Y., Cui, H. & Wang, C. Strengthening nitrogen affinity on CuAu@Cu core–shell nanoparticles with ultrathin Cu skin via strain engineering and ligand effect for boosting nitrogen reduction reaction. *Appl. Catal. B Environ.* **288**, 119999 (2021).
117. Li, C. *et al.* Sulfur vacancies in ultrathin cobalt sulfide nanoflowers enable boosted electrocatalytic activity of nitrogen reduction reaction. *Chem. Eng. J.* **415**, 129018 (2021).
118. Zhang, W. *et al.* Working-in-tandem mechanism of multi-dopants in enhancing electrocatalytic nitrogen reduction reaction performance of carbon-based materials. *Nano Res.* **14**, 3234–3239 (2021).
119. Lv, X.-W., Liu, Y., Wang, Y.-S., Liu, X.-L. & Yuan, Z.-Y. Encapsulating vanadium nitride nanodots into N,S-codoped graphitized carbon for synergistic electrocatalytic nitrogen reduction and aqueous Zn-N2 battery. *Appl. Catal. B Environ.* **280**, 119434 (2021).
120. Yang, X. *et al.* Molecular single iron site catalysts for electrochemical nitrogen fixation under ambient conditions. *Appl. Catal. B Environ.* **285**, 119794 (2021).
121. Wang, M. *et al.* Salting-out effect promoting highly efficient ambient ammonia synthesis. *Nat. Commun.* **12**, 3198 (2021).
122. Lu, K. *et al.* Synergistic Multisites Fe2Mo6S8 Electrocatalysts for Ambient Nitrogen Conversion to Ammonia. *ACS Nano* **15**, 16887–16895 (2021).
123. Wan, Y. *et al.* Oxidation State Modulation of Bismuth for Efficient Electrocatalytic Nitrogen Reduction to Ammonia. *Adv. Funct. Mater.* **31**, 2100300 (2021).

124. Hu, X. *et al.* Identifying electrocatalytic activity and mechanism of Ce1/3NbO3 perovskite for nitrogen reduction to ammonia at ambient conditions. *Appl. Catal. B Environ.* **280**, 119419 (2021).
125. Cai, W. *et al.* The twinned Pd nanocatalyst exhibits sustainable NRR electrocatalytic performance by promoting the desorption of NH3. *J. Mater. Chem. A* **9**, 13483–13489 (2021).
126. Yin, S. *et al.* Engineering One-Dimensional AuPd Nanospikes for Efficient Electrocatalytic Nitrogen Fixation. *ACS Appl. Mater. Interfaces* **13**, 20233–20239 (2021).
127. Xia, J. *et al.* Electrospun zirconia nanofibers for enhancing the electrochemical synthesis of ammonia by artificial nitrogen fixation. *J. Mater. Chem. A* **9**, 2145–2151 (2021).
128. Wang, X., Luo, M., Lan, J., Peng, M. & Tan, Y. Nanoporous Intermetallic Pd3Bi for Efficient Electrochemical Nitrogen Reduction. *Adv. Mater.* **33**, 2007733 (2021).
129. Liu, P.-Y. *et al.* Enhanced electrocatalytic nitrogen reduction reaction performance by interfacial engineering of MOF-based sulfides FeNi2S4/NiS hetero-interface. *Appl. Catal. B Environ.* **287**, 119956 (2021).
130. Chen, J. *et al.* The activation of porous atomic layered MoS2 basal-plane to induce adjacent Mo atom pairs promoting high efficiency electrochemical N2 fixation. *Appl. Catal. B Environ.* **285**, 119810 (2021).
131. Patil, S. B. *et al.* Enhanced N2 affinity of 1T-MoS2 with a unique pseudo-six-membered ring consisting of N–Li–S–Mo–S–Mo for high ambient ammonia electrosynthesis performance. *J. Mater. Chem. A* **9**, 1230–1239 (2021).
132. Li, Y. *et al.* Boosting Electroreduction Kinetics of Nitrogen to Ammonia via Tuning Electron Distribution of Single-Atomic Iron Sites. *Angew. Chem. Int. Ed.* **60**, 9078–9085 (2021).
133. Lv, X.-W., Liu, X.-L., Suo, Y.-J., Liu, Y.-P. & Yuan, Z.-Y. Identifying the Dominant Role of Pyridinic-N–Mo Bonding in Synergistic Electrocatalysis for Ambient Nitrogen Reduction. *ACS Nano* **15**, 12109–12118 (2021).
134. Zhao, Z. *et al.* Metal-Free C3N4 with plentiful nitrogen vacancy and increased specific surface area for electrocatalytic nitrogen reduction. *J. Energy Chem.* **60**, 546–555 (2021).
135. Qiu, W. *et al.* Precise synthesis of Fe–N2 with N vacancies coordination for boosting electrochemical artificial N2 fixation. *Appl. Catal. B Environ.* **293**, 120216 (2021).

136. Shang, Z. *et al.* Atomically Dispersed Manganese Lewis Acid Sites Catalyze Electrohydrogenation of Nitrogen to Ammonia. *CCS Chem.* **0**,.
137. Zhang, D. *et al.* Double-Phase Heterostructure within Fe-Doped Cu2–xS Quantum Dots with Boosted Electrocatalytic Nitrogen Reduction. *ACS Sustain. Chem. Eng.* **9**, 2844–2853 (2021).
138. Jiang, T. *et al.* Ultra-thin shelled Cu2-xS/MoS2 quantum dots for enhanced electrocatalytic nitrogen reduction. *Chem. Eng. J.* **426**, 130650 (2021).
139. Chu, K. *et al.* Amorphous MoS3 enriched with sulfur vacancies for efficient electrocatalytic nitrogen reduction. *J. Energy Chem.* **53**, 132–138 (2021).
140. Kong, Y. *et al.* Atomically Dispersed Zinc(I) Active Sites to Accelerate Nitrogen Reduction Kinetics for Ammonia Electrosynthesis. *Adv. Mater.* **34**, 2103548 (2022).
141. Shen, P. *et al.* High-Efficiency N2 Electroreduction Enabled by Se-Vacancy-Rich WSe2–x in Water-in-Salt Electrolytes. *ACS Nano* (2022) doi:10.1021/acsnano.2c00596.
142. Lazouski, N., Schiffer, Z. J., Williams, K. & Manthiram, K. Understanding Continuous Lithium-Mediated Electrochemical Nitrogen Reduction. *Joule* **3**, 1127–1139 (2019).
143. Ma, X., Zhang, Q., Gao, L., Zhang, Y. & Hu, C. Atomic-layer-deposited oxygen-deficient TiO2 on carbon cloth: an efficient electrocatalyst for nitrogen fixation. *ChemCatChem* **n/a**,.
144. Ma, C., Zhang, Y., Yan, S. & Liu, B. Carbon-doped boron nitride nanosheets: A high-efficient electrocatalyst for ambient nitrogen reduction. *Appl. Catal. B Environ.* **315**, 121574 (2022).
145. Li, K. *et al.* Increasing Current Density of Li-Mediated Ammonia Synthesis with High Surface Area Copper Electrodes. *ACS Energy Lett.* **7**, 36–41 (2022).
146. Zhao, X., Pachfule, P. & Thomas, A. Covalent organic frameworks (COFs) for electrochemical applications. *Chem. Soc. Rev.* **50**, 6871–6913 (2021).
147. Guo, W., Zhang, K., Liang, Z., Zou, R. & Xu, Q. Electrochemical nitrogen fixation and utilization: theories, advanced catalyst materials and system design. *Chem. Soc. Rev.* **48**, 5658–5716 (2019).
148. Skúlason, E. *et al.* A theoretical evaluation of possible transition metal electro-catalysts for N2 reduction. *Phys. Chem. Chem. Phys.* **14**, 1235–1245 (2011).

149. Choi, C. *et al.* Suppression of Hydrogen Evolution Reaction in Electrochemical N_2 Reduction Using Single-Atom Catalysts: A Computational Guideline. *ACS Catal.* **8**, 7517–7525 (2018).